Inorganic Chemistry

Article

pubs.acs.org/IC

Structural Study on 2,2′-(Methylimino)bis(*N*,*N*-Dioctylacetamide) Complex with $Re(VII)O_4^-$ and $Tc(VII)O_4^-$ by ^1H NMR, EXAFS, and IR Spectroscopy

Morihisa Saeki*

Quantum Beam Science Directorate, Japan Atomic Energy Agency, Tokai-mura, Naka-gun, Ibaraki 319-1195, Japan

Yuji Sasaki

Nuclear Science and Engineering Directorate, Japan Atomic Energy Agency, Tokai-mura, Naka-gun, Ibaraki 319-1195, Japan

Ayaka Nakai and Akira Ohashi

College of Science, Ibaraki University, Bunkyo 2-1-1, Mito, Ibaraki 310-8512, Japan

Dipanjan Banerjee, Andreas C. Scheinost, and Harald Foerstendorf

Helmholtz-Zentrum Dresden-Rossendorf, Institute of Resource Ecology, P.O. Box 510119, 01314 Dresden, Germany

ABSTRACT: The structures of the complex of 2,2′-(methylimino)bis(*N*,*N*-dioctylacetamide) (MIDOA) with $M(VII)O_4^-$ (M = Re and Tc), which were prepared by liquid–liquid solvent extraction, were investigated by using ^1H nuclear magnetic resonance (NMR), extended X-ray absorption fine structure (EXAFS), and infrared (IR) spectroscopy. The ^1H NMR spectra of the complex of MIDOA with $Re(VII)O_4^-$ prepared in the organic solution suggest the transfer of a proton from aqueous to organic solution and the formation of the H^+MIDOA ion. The EXAFS spectra of the complexes of H^+MIDOA with $Re(VII)O_4^-$ and $Tc(VII)O_4^-$ show only the M–O coordination of the aquo complexes, suggesting that the chemical state of $M(VII)O_4^-$ was unchanged during the extraction process. The results from ^1H NMR and EXAFS, therefore, provide evidence of $M(VII)O_4^-\cdots H^+$MIDOA complex formation in the organic solution. The IR spectra of $Re(VII)O_4^-\cdots H^+$MIDOA and $Tc(VII)O_4^-\cdots H^+$MIDOA were analyzed based on the structures and the IR spectra that were calculated at the B3LYP/cc-pVDZ level. Comparison of the observed and calculated IR spectra demonstrates that an intramolecular hydrogen bond is formed in H^+MIDOA, and the $M(VII)O_4^-$ ion interacts with H^+MIDOA through multiple $C-H_n\cdots O$ hydrogen bonds.

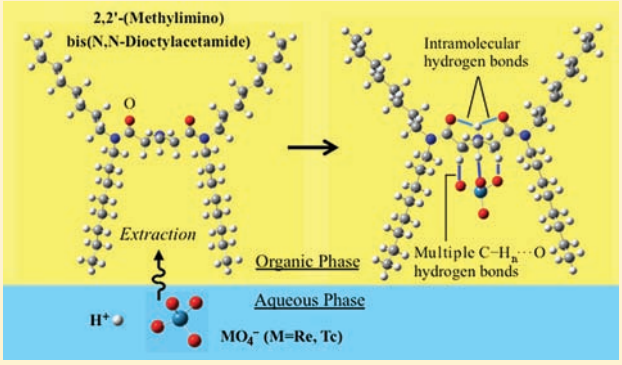

INTRODUCTION

Technetium is an artificial radioelement with a low atomic number ($Z = 43$) and a half-life of 2.1×10^5 year for the ground state of ^{99}Tc and 6.0 h for the metastable state ^{99m}Tc.[1] The ^{99}Tc is produced in appreciable amounts by fission of nuclear fuel,[2] while ^{99m}Tc is one of the most widely used radionuclides in nuclear medicine.[1] ^{99}Tc typically occurs as the oxyanion, $Tc(VII)O_4^-$, in aqueous solution under oxidizing conditions. The $Tc(VII)O_4^-$ ion has high mobility in geological environments and shows only weak interaction with inorganic solids.[3] Thus, in the concept of geological disposal of fission products, Tc is one of the key elements to be separated for the reduction of long-term radiotoxicity. One ordinary method to separate Tc from the fission products is by liquid–liquid solvent extraction. For an efficient separation using the liquid–liquid solvent extraction process, Tc-specific oxyanion receptors have to be developed.

In coordination chemistry, molecular recognition concepts have been constructed for the oxyanions, such as phosphates and sulfate.[4−7] A similar concept might be applicable to $Tc(VII)O_4^-$. The oxyanion receptors are classified into positively charged and electro-neutral hosts. In the positively charged host, the protonated receptor molecules interact with the oxyanion through electrostatic interaction supported by hydrogen bonding. As positively charged hosts, azonia,[8−13]

Received: February 14, 2012
Published: May 1, 2012

   dx.doi.org/10.1021/ic3003405 | *Inorg. Chem.* 2012, 51, 5814–5821

oligopyrrole-derived,[14,15] ammonia-based,[16] and guanidium-based receptors[17,18] have been developed. The electro-neutral hosts are further classified into receptors containing poly Lewis acids and those operating via ion-dipole binding. In the case of poly Lewis acid receptors,[19−21] a defined number and type of Lewis acids are incorporated into a molecular skeleton with their electron-deficient sites and exposed for interaction with the lone electron pairs of anions. In the receptor operating via ion-dipole binding, the hydrogen bonding plays an important role as represented in urea-based[22,23] and amide-based[24] hosts. In addition to these species, a macrotricyclic tertiary amine,[25] where the oxyanion is trapped in the cavity surrounded by a dipole-moment field, also belongs to the receptors operating with ion-dipole binding.

As a receptor for $Tc(VII)O_4^-$, quaternary (propyl, butyl, and hexyl) amine,[26] trioctylamine,[27] and methyltrioctylammonium[28] were reported. They can be classified under the ammonia-based receptors. On the other hand, 2,2′-(methylimino)bis(*N*,*N*-dioctylacetamide) (MIDOA; shown in Figure 1a) was recently found to be a compatible receptor for

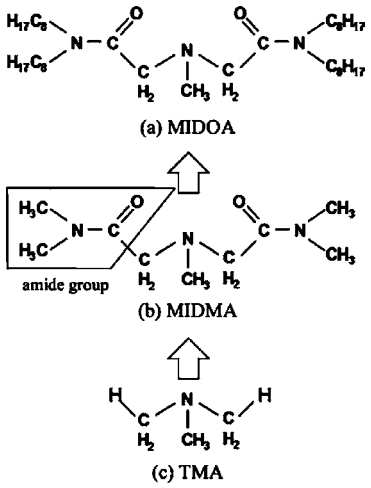

Figure 1. Chemical formulas of (a) MIDOA, (b) MIDMA, and (c) TMA.

$Tc(VII)O_4^-$ in the liquid−liquid extraction.[29−31] The MIDOA molecule is obtained by replacing methyl groups with octyl groups in 2,2′-(methylimino)bis(*N*,*N*-dimethylacetamide) (MIDMA; shown in Figure 1b), which is derived from trimethylamine (TMA; Figure 1c) by replacing terminal hydrogen atoms with amide groups. The MIDOA molecule has a high ability for complexation with the $Tc(VII)O_4^-$ ion; the distribution ratio between the organic and the aqueous phase is $>10^3$ in various extraction systems.[30]

The MIDOA molecule fundamentally belongs to the ammonia-based receptors, because it is a derivative of TMA. However, the MIDOA molecule also can be classified into the amide-based receptors because of its amide groups. Thus, only from the structure, the molecular interaction of MIDOA with $Tc(VII)O_4^-$ is unclear. Dependence of the distribution ratio of $Tc(VII)O_4^-$ on the concentration of MIDOA suggests that one $Tc(VII)O_4^-$ ion is extracted by one MIDOA molecule.[29] In addition, assuming that (i) the $Tc(VII)O_4^-\cdots H^+$MIDOA complex, where H^+MIDOA represents protonated MIDOA, is formed in the organic phase and (ii) the chemical state of $Tc(VII)O_4^-$ remains unaltered during the extraction process, the equation of extraction equilibrium from the aqueous phase to the organic phase can be described as

$$Tc(VII)O_4^- + H^+ + MIDOA \rightarrow Tc(VII)O_4^-\cdots H^+MIDOA \quad (1)$$

The $Re(VII)O_4^-$ ion is often used as a substitute for $Tc(VII)O_4^-$, because chemical properties of Re are supposed to be similar to those of Tc.[32] Moreover, the MIDOA molecule is also a good receptor for $Re(VII)O_4^-$.[29] In this work, structures of the complex of MIDOA with $M(VII)O_4^-$ (M = Re and Tc) were investigated by using ^1H nuclear magnetic resonance (NMR), extended X-ray absorption fine structure (EXAFS), and infrared (IR) spectroscopy. In case crystals can be precipitated from the liquid sample, the structure can be determined by X-ray diffraction, as for the complex of 2,2′-(methylimino)bis(*N*,*N*-diethylacetamide) (MIDEA) with $Re(VII)O_4^-$.[33] For the complex of MIDOA with $M(VII)O_4^-$, however, the crystallization process distorts the position of the H^+ ion, which plays a crucial role for the interaction between MIDOA and $M(VII)O_4^-$. Thus, we studied the structures of this complex in the organic solution without the crystallization.

First, we recorded the ^1H NMR spectrum of the complex of MIDOA with $Re(VII)O_4^-$ to verify the formation of H^+MIDOA. Subsequently, the chemical states of $Re(VII)O_4^-$ and $Tc(VII)O_4^-$ during the extraction process were investigated by EXAFS spectroscopy. In addition, the structures of the complexes of MIDOA with $Re(VII)O_4^-$ and $Tc(VII)O_4^-$ were studied by IR spectroscopy. The observed IR spectra were analyzed based on the molecular structures and IR spectra that were calculated by density functional theory (DFT). The IR spectra and the DFT calculation elucidate the structures of the $Re(VII)O_4^-\cdots H^+$MIDOA and $Tc(VII)O_4^-\cdots H^+$MIDOA complexes and the formula of intermolecular interaction.

EXPERIMENTAL AND COMPUTATIONAL METHODS

CAUTION! ^{99}Tc is a low-energy β-emitter with a half-life of 2.1×10^5 years. Appropriate radiation safety procedures were used at all times by personnel trained in the safe handling of radioactivity.

Preparation of Solutions. The $Re(VII)O_4^-$ solution was prepared by diluting 65−70 wt % $HReO_4$ stock solution (Sigma Aldrich, 99.99%) with distilled water, while $Tc(VII)O_4^-$ solution was prepared by dissolving $KTc(VII)O_4$ (Eckert & Ziegler Isotope Products, Inc.) into HCl or DCl solution. The solutions of $Re(VII)O_4^-$ and $Tc(VII)O_4^-$ were adjusted to pH 0.8. The synthesis of the MIDOA extractant, which is liquid at room temperature, is already described in ref 29. The solution of MIDOA was prepared by dissolving MIDOA into the respective organic solvent adequate for the measurements: chloroform-*d* ($CDCl_3$, Wako Chemical, 99.7%) for ^1H NMR, dodecane ($C_{12}H_{26}$, Sigma Aldrich, ≥99%) for EXAFS, and tetrachlorocarbon (CCl_4, Sigma Aldrich, 99.9%) for the IR spectroscopy.

Liquid−Liquid Solvent Extraction. The solvent extraction was performed by shaking a mixture of the 200 mM HCl or DCl solution of 5−20 mM $M(VII)O_4^-$ with the $CDCl_3$, $C_{12}H_{16}$, or CCl_4 solutions of 100 mM MIDOA at room temperature. In this operation, the complex of $M(VII)O_4^-$ and MIDOA is formed in the organic phase. After shaking for 2 h, the mixture was centrifuged to separate aqueous and organic phases. The organic solution was separated and further investigated. The acidic solution of $M(VII)O_4^-$ shows a vibrational band at 917 cm^{-1} for Re and at 905 cm^{-1} for Tc. Comparing the IR spectra of acidic solutions of $M(VII)O_4^-$ before and after the solvent extraction, we confirmed complete disappearance of the vibrational band under all extraction conditions, which indicates that the $M(VII)O_4^-$ ion is completely extracted from the aqueous phase.

dx.doi.org/10.1021/ic3003405 | *Inorg. Chem.* 2012, 51, 5814−5821

Instrumentation and Measurements. The ^{1}H NMR spectra were recorded on a Bruker Avance III 400 MHz spectrometer. Chemical shifts are referenced to internal solvent resonances and are reported relative to tetramethyl-silane.

The EXAFS measurements were performed at the Rossendorf Beamline (ROBL) at the European Synchrotron Radiation Facility (ESRF), Grenoble, under dedicated operating conditions (6 GeV; 200 mA). A Si(111) double-crystal monochromator was employed in channel-cut mode to monochromatize the white X-ray beam from the synchrotron. The organic solution of the complex of $M(VII)O_4^-$ with MIDOA was prepared in polyethylene cuvettes with a volume of 2−4 mL. Absorption spectra at the Re L_{III}-edge (10.535 keV) and the ^{99}Tc K-edge (21.044 keV) were measured in transmission mode by using Ar-filled ionization chambers at ambient temperature and pressure. Energy calibration of the measured spectra was achieved by the simultaneous measurement of Mo (20.000 keV) and Zn references (9.659 keV). Energy calibration and averaging of three scans per sample were done in SixPack, and EXAFS data extraction and shell fits were done with WinXAS and FEFF 8.2 programs. The fits were performed in R-space, and the amplitude reduction factor S_0^2 was fixed to 0.9.

The IR spectra of the MIDOA complexes in organic solution were measured with an FT-IR spectrometer of (Spectrum GX2000, Perkin-Elmer) equipped with a mercury cadmium telluride (MCT) detector or an FT-IR spectrometer of (FT/IR-4100, JASCO) equipped with a deuterated L-alanine-doped triglycine sulfate (DLATGS). The spectral resolution was 1 cm^{-1}, and spectra were averaged over 64 scans. In ATR measurement, the used accessories were a ZnSe crystal (46 mm ×12 mm) with 12 internal reflections for the spectral region of 1800−2800 cm^{-1} and a horizontal diamond crystal (diameter, 4 mm) with nine reflections for the regions of 800−1800 and 2800−3800 cm^{-1}. The entire instrument and the ATR cell were purged with a current of dry air. In the liquid membrane technique, ZnSe plates were used as cell windows.

DFT Calculation. The geometries, Gibbs free energies, enthalpy, and IR spectra of the complex of MIDOA with $M(VII)O_4^-$ were calculated at B3LYP/cc-pVDZ level using the Gaussian09 program.[34] In the geometrical optimization process, the stability of the optimized structures was checked by a harmonic frequency analysis. Most of the computations were carried out on Fujitsu PrimeQuest and Hitachi SR16000 computers at the Research Center for Computational Science, Okazaki, Japan.

RESULTS AND DISCUSSION

^{1}H NMR Spectra of Complex of MIDOA with $Re(VII)O_4^-$. Figure 2a,b shows the ^{1}H NMR spectra of the $CDCl_3$ solutions of MIDOA after extraction of the 20 mM $Re(VII)O_4^-$ ion from the HCl and DCl solutions, respectively. On the basis of the chemical shift and the splitting, we assigned the observed band as shown in Table 1. From Figure 2a to 2b, the chemical shift of H(a) and H(b) increases by 0.05−0.09 ppm, while the resonance bands of H(c), H(d), and H(e) keep their positions. The H(a) and H(b) atoms belong to methyl and methylene groups next to the central N atom. Thus, the difference in chemical shift of H(a) and H(b) suggests that the H^+ and D^+ ions are transferred from aqueous to organic phase and are bound to the N moiety in MIDOA that is neighboring the CH_3(a) and CH_2(b) groups. Thus, we are assured that the H^+MIDOA ion is formed in the extraction of $M(VII)O_4^-$.

Figure 2c shows the ^{1}H NMR spectrum of the $CDCl_3$ solution of MIDOA after extraction from the HCl solution without $Re(VII)O_4^-$. The extraction results in a transfer of the H^+ and Cl^- ions from aqueous solution and formation of the complex of H^+MIDOA with Cl^- in the $CDCl_3$ solution. The ^{1}H NMR spectrum of the complex of H^+MIDOA and Cl^- (Figure 2c) is similar to that of H^+MIDOA and $Re(VII)O_4^-$ (Figure 2a). In contrast, the resonance bands of H(a) and H(b) of the

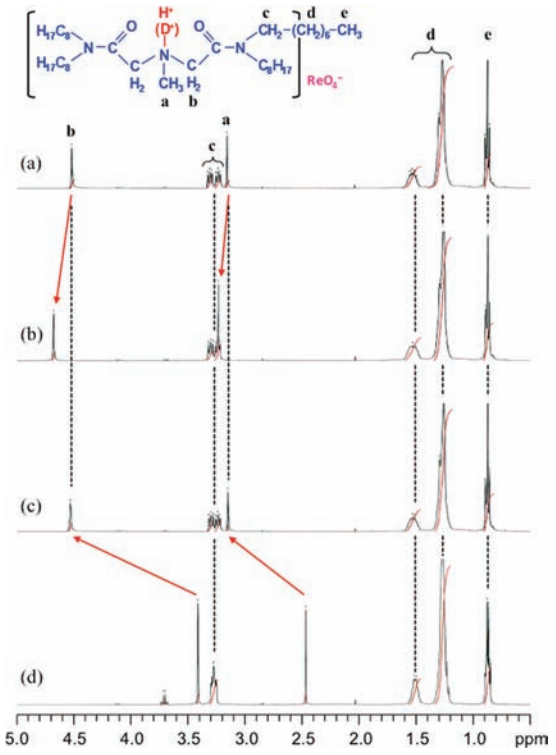

Figure 2. ^{1}H NMR spectra of MIDOA (in $CDCl_3$) after extraction from (a) the HCl solution of $Re(VII)O_4^-$, (b) the DCl solution of $Re(VII)O_4^-$, and (c) the HCl solution without $Re(VII)O_4^-$ and that of (d) MIDOA (in $CDCl_3$) before extraction. The resonance bands are labeled a−e.

Table 1. Observed Chemical Shifts (ppm) of the ^{1}H NMR Spectra of the Samples in Figure 2

sample	(a)	(b)	(c)	(d)
H(a)	3.16	3.21	3.15	2.47
H(b)	4.52	4.61	4.54	3.42
H(c)	3.30, 3.24	3.30, 3.24	3.30, 3.24	3.28
H(d)	1.54, 1.27	1.54, 1.27	1.54, 1.27	1.54, 1.27
H(e)	0.88	0.88	0.88	0.88

H^+MIDOA complexes (Figure 2a,c) largely shift from those of MIDOA before the extraction (Figure 2d) to lower magnetic field by 0.68 and 1.12 ppm. These results suggest that the electronic and geometrical structure of MIDOA is changed by the formation of H^+MIDOA, while that of H^+MIDOA is hardly affected by the coordination of the Cl^- and $Re(VII)O_4^-$ ions.

EXAFS Spectra of MIDOA Complex with $Re(VII)O_4^-$ and $Tc(VII)O_4^-$. XANES spectra of the $C_{12}H_{16}$ solution of MIDOA following extraction of 5 mM $Re(VII)O_4^-$ and $Tc(VII)O_4^-$ are shown in Figure 3a,b, along with their free aquo complexes (in red). The white line positions for Re and Tc, as well as the pre-edge, are in line with the heptavalent oxidation state. Furthermore, the shape of XANES does not change by the complexation with MIDOA, indicating that the coordination geometry remains the same as for the aquo complex. EXAFS spectra of MIDOA complexes of $Re(VII)O_4^-$ and $Tc(VII)O_4^-$ are displayed in Figure 3c,d, respectively. Figure 3e,f exhibit the corresponding Fourier transform magnitude (FTM). As it is apparent from the FTM, all EXAFS spectra are dominated by the M(VII)−O coordination shell (FTM peak at about 1.3 Å, uncorrected for phase shift)

dx.doi.org/10.1021/ic3003405 | Inorg. Chem. 2012, 51, 5814−5821

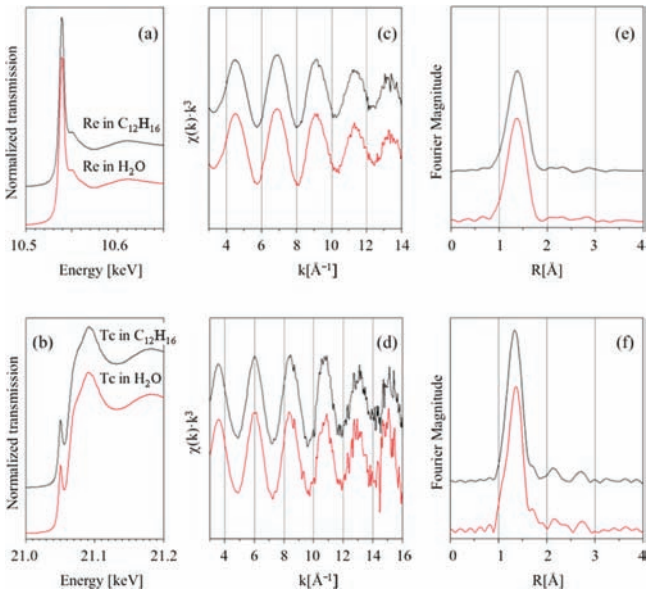

Figure 3. XANES spectra of MIDOA complexes in $C_{12}H_{16}$ of (a) $Re(VII)O_4^-$ and (b) $Tc(VII)O_4^-$, EXAFS spectra of (c) $Re(VII)O_4^-$ and (d) $Tc(VII)O_4^-$ and corresponding FTM for (e) $Re(VII)O_4^-$ and (f) $Tc(VII)O_4^-$. The corresponding aquo complexes are shown in red for $Re(VII)O_4^-$ and $Tc(VII)O_4^-$.

and show no difference between the aquo and the MIDOA complexes.

Coordination numbers (CNs), radial distances (R), and Debye–Waller factors (σ^2) were obtained by shell fitting based on the structural models of $KTcO_4$ and $KReO_4$[35] and are shown in Table 2. The uncertainties of these values are ±0.5 for

Table 2. Coordination Number (CN), Radial Distance (R), and Debye–Waller Factor (σ^2) of the Re–O and Tc–O Coordinations

	CN	R (Å)	σ^2 (Å^2)
ReO_4^- in HCl	4.2	1.74	0.0031
complex of MIDOA with Re(VII)	4.4	1.73	0.0034
TcO_4^- in HCl	4.0	1.72	0.0014
complex of MIDOA with Tc(VII)	3.8	1.73	0.0013

CN, ± 0.005 Å for R, and ±0.0005 Å^2 for σ^2. The bond distances of Re–O (1.74 Å) and Tc–O (1.72 Å) in the HCl solution agree well with previous studies.[36−38] The Re and Tc ions are dissolved in the HCl solution as $Re(VII)O_4^-$ and $Tc(VII)O_4^-$, which is reflected by CN = 4 with its uncertainty in Table 2. The CN values remain 4 in the complex of MIDOA with M(VII) as well and indicate that their chemical states are also unaltered during the extraction process. Note two small FTM peaks at 2.1 and 2.7 Å in Figure 3f, which are present in both the aquo and the MIDOA complex, hence cannot be due to backscattering from atoms of MIDOA. They arise in fact from 3-legged and 4-legged multiple scattering contributions from the Tc–O shell, respectively. Such multiple scattering contributions are not apparent for Re, which can be explained by the higher static and/or vibrational disorder of the ReO_4 unit (see σ^2 in Table 2). Therefore, the MIDOA complexes with $Re(VII)O_4^-$ and $Tc(VII)O_4^-$ are structurally not different from the pure aquo complexes within the structural range of the EXAFS method (approximately 4 Å around the metal centers).

IR Study of $Re(VII)O_4^-\cdots H^+$MIDOA and $Tc(VII)O_4^-\cdots H^+$MIDOA Complexes. The ^{1}H NMR and EXAFS results validate the hypothesis of eq 1 and the formation of the $M(VII)O_4^-\cdots H^+$MIDOA complexes. In the next step, we investigated the structure of $M(VII)O_4^-\cdots H^+$MIDOA by ATR FT-IR spectroscopy. Figure 4a–c displays the mid-IR spectra of

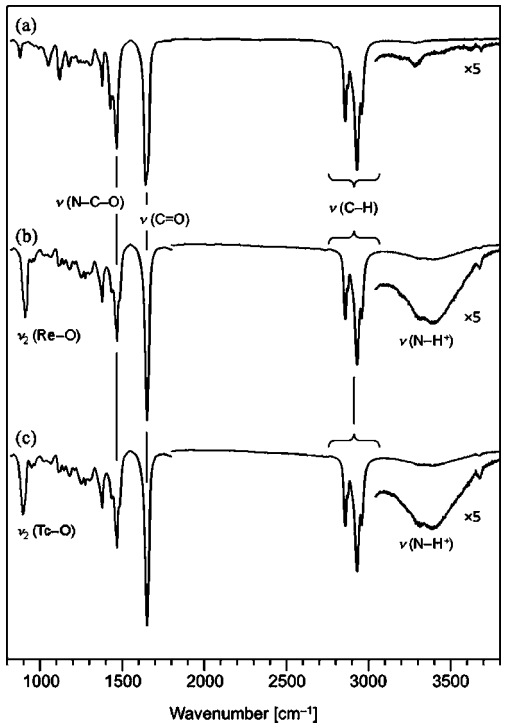

Figure 4. IR spectra of (a) MIDOA, (b) $Re(VII)O_4^-\cdots H^+$MIDOA, and (c) $Tc(VII)O_4^-\cdots H^+$MIDOA (in CCl_4).

MIDOA, the $Re(VII)O_4^-\cdots H^+$MIDOA, and the $Tc(VII)O_4^-\cdots H^+$MIDOA complexes in CCl_4, respectively. The vibrational bands of CCl_4 and H_2O/CO_2 in air were subtracted as background correction. Several bands in Figure 4a–c are assigned based on the IR spectrum database,[39] as listed in Table 3.

Table 3. Observed IR Frequencies (cm^{-1}) of Main Vibrational Bands of MIDOA, $Re(VII)O_4^-\cdots H^+$MIDOA, and $Tc(VII)O_4^-\cdots H^+$MIDOA

	MIDOA	Re(VII) $O_4^-\cdots H^+$MIDOA	Tc(VII) $O_4^-\cdots H^+$MIDOA
ν_3(M–O)		910	896
ν(N–C=O)	1467	1467	1467
ν(C=O)	1643	1652	1652
ν(C–H)	2857, 2929, 2958	2857, 2929, 2958	2857, 2929, 2958
ν(N–H$^+$)		~3400	~3400

In the IR spectrum of 100 mM MIDOA (Figure 4a), the bands in the region of 900–1400 cm^{-1} can be assigned to C–C and C–N stretching modes and bending modes of X–C–Y (X = H, C, and N; Y = H, C, N, and O). The vibrational band at 1467 cm^{-1} is attributed to the bending mode of the N–C=O group, while the bands at 1643 and 2850–3000 cm^{-1} are assigned to stretching modes of C=O and C–H, respectively.

dx.doi.org/10.1021/ic3003405 | Inorg. Chem. 2012, 51, 5814–5821

Besides the bands of MIDOA, IR spectra of 20 mM $Re(VII)O_4^-\cdots H^+$MIDOA and $Tc(VII)O_4^-\cdots H^+$MIDOA (Figure 4b,c) show the appearance of a sharp band around 900 cm^{-1} and a broad one centering at 3400 cm^{-1}. The sharp bands at 910 cm^{-1} found for $Re(VII)O_4^-\cdots H^+$MIDOA and at 896 cm^{-1} for $Tc(VII)O_4^-\cdots H^+$MIDOA are assigned to the ν_3 antisymmetric stretching mode of $M(VII)O_4^-$. These modes are red-shifted by approximately 7–9 cm^{-1} as compared to those of the uncomplexed anions observed in aqueous solution, which are at 917 cm^{-1} for Re(VII) and at 905 cm^{-1} for Tc(VII). The red shift is assumed to arise from the intermolecular interactions between MIDOA and $M(VII)O_4^-$.

The broad band around 3400 cm^{-1} is assigned to the hydrogen-bonded stretching mode of $N-H^+$ in H^+MIDOA. To test this assignment, we prepared the $Re(VII)O_4^-\cdots D^+$MIDOA complex by the extraction of $Re(VII)O_4^-$ from the DCl solution and recorded its spectrum by the liquid membrane technique. The IR spectra of $Re(VII)O_4^-\cdots H^+$MIDOA and $Re(VII)O_4^-\cdots D^+$MIDOA are shown in Figure 5. A comparison

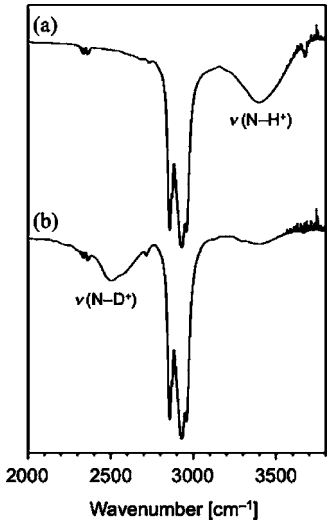

Figure 5. IR spectra of (a) $Re(VII)O_4^-\cdots H^+$MIDOA and (b) $Re(VII)O_4^-\cdots D^+$MIDOA (in CCl_4).

of two complexes clearly demonstrates the disappearance of the band around 3400 cm^{-1} and reappearance of a broad band around 2600 cm^{-1} upon deuteration of the Re(VII)–MIDOA complex, which confirms the assignment of the broad band to the $\nu(N-H^+)$ mode.

Calculated Structure of the $Re(VII)O_4^-\cdots H^+$MIDOA Complex. Prior to geometrical optimization of $Re(VII)O_4^-\cdots H^+$MIDOA, we investigated the stable structures of $Re(VII)O_4^-$ complexed with H^+MIDMA (refer to Figure 1b), representing a simplified analogue to MIDOA. Structures of the $Re(VII)O_4^-\cdots H^+$MIDOA complex were optimized from initial geometries by replacing the methyl groups in $Re(VII)O_4^-\cdots H^+$MIDMA with octyl groups.

Figure 6 shows the stable structures of $Re(VII)O_4^-\cdots H^+$MIDOA with first, second, and third lowest electronic energy, together with structural formula around central part of the complex. Geometrical parameters of the isomers **a**–**c** are listed in Table 4. The $Re(VII)O_4^-$ ion interacts with H^+MIDOA through multiple $C-H_n\cdots O$ hydrogen bonds in the isomer **a** and through an $N-H^+\cdots O$ hydrogen bond in isomers **b** and **c**. The difference between isomers **b** and **c** is the

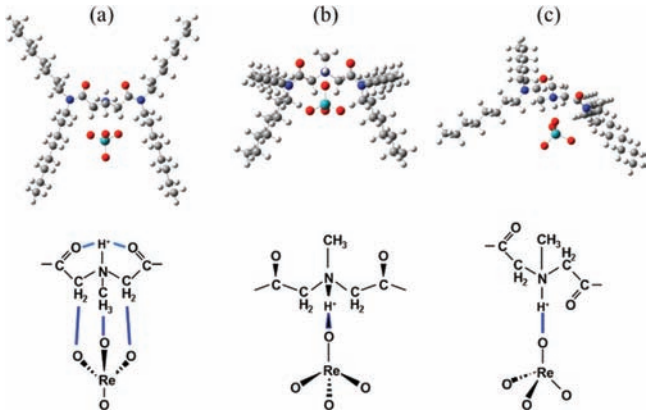

Figure 6. Calculated structures of $Re(VII)O_4^-\cdots H^+$MIDOA with first (a), second (b), and third lowest (c) electronic energy, together with structural formula of the central part of the complex. Blue lines indicate the formation of hydrogen bonds.

position of O atoms in H^+MIDOA. The averaged M–O bond length of $Re(VII)O_4^-\cdots H^+$MIDOA is 1.736 Å in every isomer. It means that the isomers **a**–**c** cannot be distinguished by the EXAFS measurement. The difference of the calculated Re–O bond length is small (0.001 Å) between the uncomplexed $Re(VII)O_4^-$ ion and the $Re(VII)O_4^-\cdots H^+$MIDOA complex in every isomer. This agrees with the trivial change of the observed radial distance of the Re–O coordination by the complex formation (Table 2).

The $Re(VII)O_4^-\cdots H^+$MIDOA complex may be formed by the following reaction,

$$Re(VII)O_4^- + H^+ + MIDOA \rightarrow Re(VII)O_4^-\cdots H^+MIDOA \quad (2)$$

Table 5 shows Gibbs free energies (ΔG_f) of reaction 2 that are calculated for isomers **a**–**c** without solvent effects at 298 K. In addition, the enthalpy values (ΔH_f) of reaction 2 in $CHCl_3$, n-$C_{12}H_{26}$, and CCl_4 were calculated by default SCRF method[40] in the Gaussian09 program and are also shown in Table 5. The ΔG_f values for complexes in the solvents were not computed because convergence of the geometrical optimization was poor in considering the solvent effect. In the future, this problem could be overcome by using refined basis sets that are not available in our computational resource at present. The ΔG_f and ΔH_f values suggest that in every case the isomer **a** has the most stable structure, although the energy difference among the isomers is below 7 kcal/mol. In H^+MIDOA of the isomer **a**, an intramolecular hydrogen bond is formed between the proton of the $N-H^+$ moiety and the O atoms of the carboxyl groups. We assume that the formation of the intermolecular hydrogen bond makes isomer **a** more stable.

Figure 7 shows the simulated IR spectra of isomers **a**–**c** obtained from B3LYP/cc-pVDZ calculation. For comparison, the experimentally obtained IR spectrum is also shown. The calculated frequencies of the isomers **a**–**c** are listed in Table 6. For isomers **a** and **b**, the hydrogen-bonded $N-H^+$ stretching mode is calculated at higher frequencies than those of the C–H stretching modes, whereas a lower frequency was calculated for isomer **c**. The result of isomer **c** disagrees with the IR spectra observed, where the $N-H^+$ stretching mode was located around 3400 cm^{-1}. Thus, isomer **c** was ruled out to represent an accurate structure of $Re(VII)O_4^-\cdots H^+$MIDOA.

dx.doi.org/10.1021/ic3003405 | Inorg. Chem. 2012, 51, 5814–5821

Table 4. Calculated Bond Lengths and Angles of Isomers a–c of $Re(VII)O_4^-\cdots H^+MIDOA$ and Isomer a of $Tc(VII)O_4^-\cdots H^+MIDOA$[a]

	$Re(VII)O_4^-\cdots H^+MIDOA$				$Tc(VII)O_4^-\cdots H^+MIDOA$	
	isomer **a**	isomer **b**	isomer **c**	ReO_4^-[b]	isomer **a**	TcO_4^-[b]
			M–O bond lengths			
free	1.721	1.723	1.719		1.704	
		1.723	1.722			
		1.748	1.741			
hydrogen bonded	1.737	1.749	1.763		1.723	
	1.739				1.725	
	1.748				1.735	
averaged[c]	1.736	1.736	1.736	1.737	1.722	1.723
	other bond lengths					
$O\cdots H_3C$[d]	2.391				2.448	
$O\cdots H_2C$[d]	2.706				2.683	
$O\cdots H^+$		1.898	1.623			
$N-H^+$	1.043	1.046	1.067		1.043	
			bond angles			
$N-H^+-O$		135	163			

[a]The M–O bond lengths of uncomplexed $Re(VII)O_4^-$ and $Tc(VII)O_4^-$ ions are also shown. The units are Å in length and degree in angle. [b]Uncomplexed MO_4^- ion. [c]Averaged value of four M–O bonds. [d]The shortest bond was selected among the several O···H bonds.

Table 5. Calculated ΔG_f Values of Isomers a–c of $Re(VII)O_4^-\cdots H^+MIDOA$ and Isomer a of $Tc(VII)O_4^-\cdots H^+MIDOA$ without Solvent Effect at 298 K for Reactions 2 and 1[a]

	$Re(VII)O_4^-\cdots H^+MIDOA$			$Tc(VII)O_4^-\cdots H^+MIDOA$
	isomer **a**	isomer **b**	isomer **c**	isomer **a**
ΔG_f	−322	−315	−319	−324
ΔH_f				
in $CHCl_3$	−227	−223	−224	−228
in n-$C_{12}H_{26}$	−271	−266	−268	−271
in CCl_4	−263	−259	−260	−264

[a]The ΔH_f values in $CHCl_3$, n-$C_{12}H_{26}$, and CCl_4 are also shown. Values are given in kcal/mol.

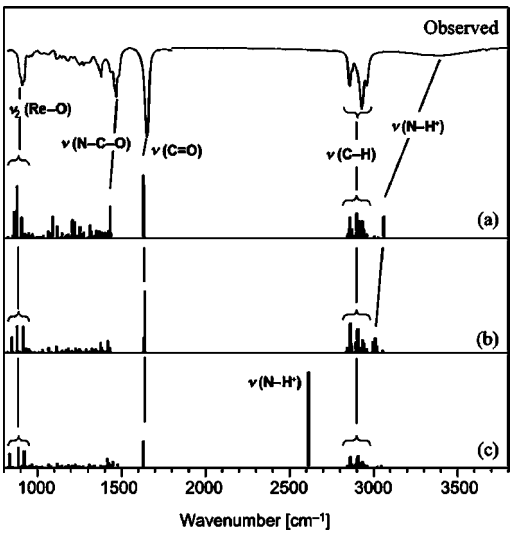

Figure 7. Simulated IR spectra of isomers **a**–**c** (Figure 6) in the B3LYP/cc-pVDZ calculation and observed IR spectrum of $Re(VII)O_4^-\cdots H^+MIDOA$.

The main difference in the simulated spectra between isomers **a** and **b** is the intensity of N–C=O bending mode, which is predicted to show a more enhanced intensity for the isomer **a** (Figure 7). In fact, the IR spectrum shows an enhanced band in this frequency range. Additionally, because isomer **a** was calculated to represent the most stable structure of the $Re(VII)O_4^-\cdots H^+MIDOA$ complex, we conclude that this isomer is the predominant species in the organic phase.

Calculated Structure of $Tc(VII)O_4^-\cdots H^+MIDOA$ Complex. The results from EXAFS (Figure 3) and IR spectroscopy (Figure 4) strongly suggest that there is hardly any difference between the overall structures of $Tc(VII)O_4^-\cdots H^+MIDOA$ and $Re(VII)O_4^-\cdots H^+MIDOA$ complexes. Thus, we assume that the structure of $Tc(VII)O_4^-\cdots H^+MIDOA$ complex is close to those of isomer **a** in Figure 6. Geometrical parameters of the optimized structure of $Tc(VII)O_4^-\cdots H^+MIDOA$ are listed in Table 4. Averaged bond lengths of Tc–O are shorter than that of Re–O by 0.015 Å. This difference was not observed in EXAFS due to the experimental uncertainty. In the same way as $Re(VII)O_4^-$, the difference of the calculated Tc–O bond length is small (0.001 Å) between $Tc(VII)O_4^-$ and $Tc(VII)O_4^-\cdots H^+MIDOA$. This agrees with the trivial change of the observed radial distance of the Tc–O coordination by the complex formation (Table 2).

The ΔG_f values calculated without solvent effects and the ΔH_f values of reaction 1 calculated for $Tc(VII)O_4^-\cdots H^+MIDOA$ in $CHCl_3$, n-$C_{12}H_{26}$, and CCl_4 are shown in Table 5. The difference of ΔG_f and ΔH_f between $Tc(VII)O_4^-\cdots H^+MIDOA$ and $Re(VII)O_4^-\cdots H^+MIDOA$ is <2 kcal/mol. The calculated frequencies of $Tc(VII)O_4^-\cdots H^+MIDOA$ are similar to those of $Re(VII)O_4^-\cdots H^+MIDOA$, except the ν_3(M–O) mode (Table 6). These results suggest the high structural similarities between the $Tc(VII)O_4^-$ and the $Re(VII)O_4^-$ complexes of MIDOA.

Relevance of the Proton in $M(VII)O_4^-\cdots H^+MIDOA$ Complexes. In the discussion above, we concluded that the isomer **a** (Figure 6) represents the predominant structure of $M(VII)O_4^-\cdots H^+MIDOA$ complex in the organic phase. In this structure, the proton does not directly contribute to the interaction between $M(VII)O_4^-$ and MIDOA. To elucidate the impact of proton on the isomer **a**, we investigated changes in the charge population upon protonation of MIDOA,

dx.doi.org/10.1021/ic3003405 | Inorg. Chem. 2012, 51, 5814–5821

Table 6. Calculated Frequencies (cm^{-1}) of IR Modes of $Re(VII)O_4^-\cdots H^+MIDOA$ (Isomers a–c) and of $Tc(VII)O_4^-\cdots H^+MIDOA$ (Isomer a) without Solvent Effect

	$Re(VII)O_4^-\cdots H^+MIDOA$			$Tc(VII)O_4^-\cdots H^+MIDOA$
	isomer a	isomer b	isomer c	isomer a
ν_3(M–O)	861, 879, 904	846, 878, 914	834, 885, 921	866, 885, 895
ν(N–C=O)	1432	1416–1429[b]	1415–1446	1432
ν(C=O)	1630, 1635	1632, 1639	1629, 1632	1629, 1635
ν(C–H)[a]	2840–3028	2838–3052	2834–3045	2840–3027
ν(N–H^+)	3060	2995–3019[b]	2611	3055

[a]Region of the calculated frequencies is shown, because there are many ν(C–H) modes. [b]Region of the calculated frequencies is shown, because the vibrational mode is coupled with several other ones.

$$H^+ + MIDOA \rightarrow H^+MIDOA \quad (3)$$

and upon formation of the complex,

$$Re(VII)O_4^- + H^+MIDOA \rightarrow Re(VII)O_4^-\cdots H^+MIDOA \quad (4)$$

by natural bond orbital (NBO) analysis,[41] as shown in Table 7. The notations used in Table 7 are explained in Figure 8. Table 7 predicts that protonation of MIDOA leads to an increase in the charge of H(a) and H(b) atoms by +0.1 and only to small changes in case of C(c), C(d) and N(e) atoms. No changes in the charge population on the atoms are expected upon formation of the complex. Considering that the H(a) and H(b) atoms directly contribute to the formation of multiple C–$H_n\cdots$O hydrogen bonds, we conclude that the increase in charge of H(a) and H(b) enhances the interactions between $Re(VII)O_4^-$ and H^+MIDOA. This discussion is also valid for the $Tc(VII)O_4^-\cdots H^+$MIDOA complex.

Table 7. Charge Population in MIDOA, H^+MIDOA, and $Re(VII)O_4^-\cdots H^+$MIDOA (Isomer a) Calculated by NBO Analysis without Solvent Effect

	MIDOA	H^+MIDOA	$Re(VII)O_4^-\cdots H^+$MIDOA
H(a) × 3	0.63	0.74	0.73
H(b) × 2	0.42	0.51	0.55
C(c)	−0.43	−0.41	−0.41
C(d)	−0.30	−0.30	−0.31
N(e)	−0.52	−0.53	−0.49

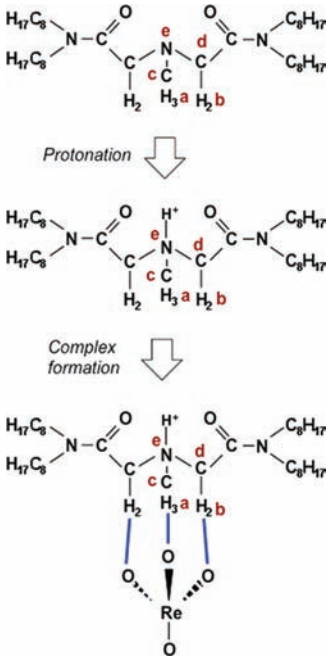

Figure 8. Scheme of protonation and complex formation of $Re(VII)O_4^-\cdots H^+$MIDOA. Blue lines indicate the formation of hydrogen bonds.

CONCLUSIONS

We prepared the MIDOA complexes with $Re(VII)O_4^-$ and $Tc(VII)O_4^-$ by the liquid–liquid solvent extraction and obtained information about their structures and chemical states from ^{1}H NMR, EXAFS, and FT-IR spectroscopy. The ^{1}H NMR spectra of the complexes, which were prepared by extraction of $Re(VII)O_4^-$ from the HCl and DCl solutions, clearly demonstrate formation of H^+MIDOA ion in the organic solution. EXAFS spectra of the complexes of H^+MIDOA with $Re(VII)O_4^-$ and $Tc(VII)O_4^-$ were exclusively dominated by M–O coordination and provide no additional information about intermolecular interaction. The coordination number of $Re(VII)O_4^-$ and $Tc(VII)O_4^-$ obtained from the EXAFS suggests that the molecular structure of $M(VII)O_4^-$ was unchanged during the extraction process. Results from ^{1}H NMR and EXAFS indicate the formation of the $M(VII)O_4^-\cdots H^+$MIDOA complex in the organic solution. Additional information on the structures of complexes was obtained by IR spectroscopy. The IR spectra of the MIDOA complexes with $Re(VII)O_4^-$ that were prepared by the HCl and DCl solution confirmed us in the formation of the $M(VII)O_4^-\cdots H^+$MIDOA complex. The IR spectra were analyzed by a comparative approach based on structures and IR spectra calculated at the B3LYP/cc-pVDZ level. The comparison of the experimental and calculated IR data suggested molecular interactions of $M(VII)O_4^-$ ions with H^+MIDOA through multiple C–$H_n\cdots$O hydrogen bonds. In addition, from charge population analysis by NBO, it was concluded that in the $M(VII)O_4^-\cdots H^+$MIDOA complex the H^+ ion does not directly contribute to intermolecular interaction but enforces the multiple C–$H_n\cdots$O hydrogen bonds by enhancement of positive charge on the H atoms.

AUTHOR INFORMATION

Corresponding Author

*Tel: +81-29-282-5500. Fax: +81-29-282-5768. E-mail: saeki.morihisa@jaea.go.jp.

Notes

The authors declare no competing financial interest.

dx.doi.org/10.1021/ic3003405 | Inorg. Chem. 2012, 51, 5814–5821

■ ACKNOWLEDGMENTS

We are thankful to Prof. Dr. Masaki Ozawa (Tokyo Institute for Technology) for his support as a project leader. We are also grateful to Prof. Dr. Yasuhisa Ikeda (Tokyo Institute for Technology) for his valuable comments, to Dr. Satoru Tsushima (HZDR) for his theoretical advice, to Karsten Heim (HZDR) for his technical support, to Dr. Hirotoshi Mori (Ochanomizu University) for his advice about the DFT calculation, to Dr. Christoph Hennig (HZDR) for his information about the Tc studies, and to Dr. Karim Fahmy (HZDR) for his comments on our paper. This work was partially supported by MEXT, Grant-in-Aid for Scientific Research (A) (21246146).

■ REFERENCES

(1) Lieser, K. H. *Radiochim. Acta* **1993**, *63*, 5−8.
(2) Kubota, M. *Radiochim. Acta* **1993**, *63*, 91−96.
(3) Lieser, K. H.; Bauscher, C. *Radiochim. Acta* **1987**, *42*, 205−213.
(4) Hay, B. P. *Chem. Soc. Rev.* **2010**, *39*, 3700−3708.
(5) Schmidtchen, F. P.; Berger, M. *Chem. Rev.* **1997**, *97*, 1609−1646.
(6) Gale, P. A.; Gunnlaugsson, T. *Chem. Soc. Rev.* **2010**, *39*, 3595−3596.
(7) Philip, A, G. *Coord. Chem. Rev.* **2003**, *240*, 1.
(8) Hosseini, M. W.; Blacker, A. J.; Lehn, J. M. *J. Am. Chem. Soc.* **1990**, *112*, 3896−3904.
(9) Hosseini, M. W.; Lehn, J. M.; Maggiora, L.; Mertes, K. B.; Mertes, M. P. *J. Am. Chem. Soc.* **1987**, *109*, 537−544.
(10) Dietrich, B.; Hosseini, M. W.; Lehn, J.-M.; Sessions, R. B. *Helv. Chim. Acta* **1983**, *66*, 1262−1278.
(11) Schmidtchen, F. P. *Chem. Ber.* **1981**, *114*, 597−607.
(12) Schmidtchen, F. P. *Chem. Ber.* **1980**, *113*, 864−874.
(13) Schmidtchen, F. P. *Angew. Chem.* **1977**, *89*, 751−752.
(14) Schmuck, C.; Bickert, V. *J. Org. Chem.* **2007**, *72*, 6832−6839.
(15) Sessler, J. L.; Camiolo, S.; Gale, P. A. *Coord. Chem. Rev.* **2003**, *240*, 17−55.
(16) Llinares, J. M.; Powell, D.; Bowman-James, K. *Coord. Chem. Rev.* **2003**, *240*, 57−75.
(17) Best, M. D.; Tobey, S. L.; Anslyn, E. V. *Coord. Chem. Rev.* **2003**, *240*, 3−15.
(18) Schmuck, C. *Coord. Chem. Rev.* **2006**, *250*, 3053−3067.
(19) Lacy, S. M.; Rudkevich, D. M.; Verboom, W.; Reinhoudt, D. N. *J. Chem. Soc., Perkin Trans. 2* **1995**, 135−139.
(20) Jacobson, S.; Pizer, R. *J. Am. Chem. Soc.* **1993**, *115*, 11216−11221.
(21) Blanda, M. T.; Newcomb, M. *Tetrahedron Lett.* **1989**, *30*, 3501−3504.
(22) Amendola, V.; Fabbrizzi, L.; Mosca, L. *Chem. Soc. Rev.* **2010**, *39*, 3889−3915.
(23) Li, A.-F.; Wang, J.-H.; Wang, F.; Jiang, Y.-B. *Chem. Soc. Rev.* **2010**, *39*, 3729−3745.
(24) Bondy, C. R.; Loeb, S. J. *Coord. Chem. Rev.* **2003**, *240*, 77−99.
(25) Worm, K.; Schmidtchen, F. P. *Angew. Chem., Int. Ed. Engl.* **1995**, *34*, 65−66.
(26) Maeck, W. J.; Booman, G. L.; Kussy, M. E.; Rein, J. E. *Anal. Chem.* **1961**, *33*, 1775−1780.
(27) Maiti, M.; Lahiri, S. *J. Radioanal. Nucl. Chem.* **2010**, *283*, 661−663.
(28) Rohal, K. M.; Seggen, D. M. V.; Clark, J. F.; McClure, M. K.; Chambliss, C. K.; Strauss, S. H.; Schroeder, N. C. *Solvent Extr. Ion Exch.* **1996**, *14*, 401−416.
(29) Sasaki, Y.; Kitatsuji, Y.; Kimura, T. *Chem. Lett.* **2007**, *36*, 1394−1395.
(30) Sasaki, Y.; Ozawa, M.; Kimura, T.; Ohashi, K. *Solvent Extr. Ion Exch.* **2009**, *27*, 378−394.
(31) Sasaki, Y.; Sugo, Y.; Saeki, M.; Morita, Y.; Ohashi, A. *Solvent Extr. Res. Dev.* **2011**, *18*, 69−74.
(32) Cotton, F. A.; Willkinson, G.; Murillo, C. A.; Bochmann, M. In *Advanced Inorganic Chemistry*, 6th ed.; Wiley-Interscience: New York, 1999; pp 974−1000.
(33) Ali, M. C.; Kawasaki, T.; Nogami, M.; Saeki, M.; Sasaki, Y.; Ikeda, Y. *Prog. Nucl. Energy* **2011**, *53*, 1005−1008.
(34) Frisch, M. J.; Trucks, G. W.; Schlegel, H. B.; Scuseria, G. E.; Robb, M. A.; Cheeseman, J. R.; Scalmani, G.; Barone, V.; Mennucci, B.; Petersson, G. A.; Nakatsuji, H.; Caricato, M.; Li, X.; Hratchian, H. P.; Izmaylov, A. F.; Bloino, J.; Zheng, G.; Sonnenberg, J. L.; Hada, M.; Ehara, M.; Toyota, K.; Fukuda, R.; Hasegawa, J.; Ishida, M.; Nakajima, T.; Honda, Y.; Kitao, O.; Nakai, H.; Vreven, T.; Montgomery, J. A., Jr.; Peralta, J. E.; Ogliaro, F.; Bearpark, M.; Heyd, J. J.; Brothers, E.; Kudin, K. N.; Staroverov, V. N.; Kobayashi, R.; Normand, J.; Raghavachari, K.; Rendell, A.; Burant, J. C.; Iyengar, S. S.; Tomasi, J.; Cossi, M.; Rega, N.; Millam, J. M.; Klene, M.; Knox, J. E.; Cross, J. B.; Bakken, V.; Adamo, C.; Jaramillo, J.; Gomperts, R.; Stratmann, R. E.; Yazyev, O.; Austin, A. J.; Cammi, R.; Pomelli, C.; Ochterski, J. W.; Martin, R. L.; Morokuma, K.; Zakrzewski, V. G.; Voth, G. A.; Salvador, P.; Dannenberg, J. J.; Dapprich, S.; Daniels, A. D.; Farkas, O.; Foresman, J. B.; Ortiz, J. V.; Cioslowski, J.; Fox, D. J. *Gaussian 09*, revision A.02; Gaussian, Inc.: Wallingford, CT, 2009.
(35) Krebs, B.; Hasse, K.-D. *Acta Crystallogr., Sect. B* **1976**, *32*, 1334−1337.
(36) Suzuki, S.; Yaita, T; Okamoto, Y.; Shiwaku, H.; Motohashi, H. *Phys. Scr.* **2005**, *T115*, 306−307.
(37) Allen, P. G.; Siemering, G. S.; Shuh, D. K.; Bucher, J. J.; Edelstein, N. M.; Langton, C. A.; Clark, S. B.; Reich, T.; Denecke, M. A. *Radiochim. Acta* **1997**, *76*, 77−86.
(38) Poineau, F.; Fattahi, M.; Auwer, C. D.; Hennig, C.; Grambow, B. *Radiochim. Acta* **2006**, *94*, 283−289.
(39) Nakamoto, K. Infrared and Raman spectra of inorganic and coordination compounds. In *Handbook of Vibrational Spectroscopy*; Chalmers, J. M., Griffiths, P., Eds.; John Wiley & Sons: Chichester, 2002; Vol. 3, pp 1872−1892.
(40) Tomasi, J.; Mennucci, B.; Cammi, R. *Chem. Rev.* **2005**, *105*, 2999−3093.
(41) Reed, A. E.; Curtiss, L. A.; Weinhold, F. *Chem. Rev.* **1988**, *88*, 899−926.